Journal of Magnetism and Magnetic Materials 467 (2018) 69–73

Contents lists available at ScienceDirect

Journal of Magnetism and Magnetic Materials

journal homepage: www.elsevier.com/locate/jmmm

Research articles

Thickness effect on magnetocrystalline anisotropy of MnPt(0 0 1) film

Qurat-ul-ain[a], Do Duc Cuong[a], Dorj Odkhuu[b], S.H. Rhim[a,*], S.C. Hong[a]

[a] Department of Physics and Energy Harvest Storage Research Center, University of Ulsan, Ulsan 44610, Republic of Korea
[b] Department of Physics, Incheon National University, Incheon 22012, Republic of Korea

ARTICLE INFO

Keywords:
Magnetocrystalline anisotropy
MnPt
Thin film
First-principles calculation
Interface

ABSTRACT

We investigated the magnetocrystalline anisotropy (MCA) of MnPt(0 0 1) film and MnPt/MgO(0 0 1) using *ab initio* electronic structure calculations. We found that the magnetic ground state of the MnPt film strongly depends on thickness (n). In bulk and in film with n ≥ 7 monolayers; AFM-II is the magnetic ground state. However, as the film thickness reduces, the magnetic ground state shifts from AFM-II to AFM-III. We employ layer-by-layer Heisenberg model to explain thickness dependent ground state transition. AFM-III state in the Mn-terminated film shows large perpendicular MCA(PMCA), which further enhances on a MgO(0 0 1) substrate. We conclude that the interface plays a key role for the enhancement of PMCA on the substrate.

1. Introduction

In recent years, there has tremendous progress and discovery in spintronics. In material perspective, most studies and applications have been focused on ferromagnetic (FM) materials [1–3], while anti-ferromagnetic (AFM) materials has been rather put aside and considered relatively useless. It is quite recent that advantages of AFM materials are recognized. Net zero magnetization produces no stray field unlike FM [4], which also implies less sensitivity to external field. Furthermore, the characteristic frequencies of switching two magnetic states in AFM's are several orders higher than typical FM materials [5–8]. This means a possibility to make high-speed devices operating not in gigahertz (as FM) but in terahertz (THz) range [9,10]. On the other hand, in property perspective, magnetocrystalline anisotropy (MCA) intrinsically associated with spin-orbit coupling (SOC) turns out to be an important ingredient in spintronics. Large MCA offers thermal stability as well as small switching current in practical applications. Summing up these, AFM with large MCA would be highly prospective as reported in several experiments [5,11,12] and also from theoretical work [13–15].

MCA can be maximized in bimetallic systems by combining high magnetic moment of a 3*d* transition metal with large SOC of a 5*d* transition metal [16–21]. MnPt alloy is an AFM material with high Néel temperature T_N = 700 °C [17], an ideal system that naturally combines high magnetic moment with large SOC. It crystallizes in CuAu-I type tetragonal crystal ($L1_0$) structure, where shows spin-reorientation in highly ordered single crystals. The spin axis shifts to *a-b* plane from *z*-axis upon heating across the temperature around 440 °C [17–20]. Heating across this temperature changes structure and magnetism.

In this article, the thickness and the surface-termination dependent magnetism along with MCA's of MnPt (0 0 1) thin films in different magnetic orderings were thoroughly investigated. Thickness of the film significantly affects the magnetism. For a Mn-terminated film, ground state shifts from AFM-II to AFM-III for film thickness n < 7 monolayers (ML). For a Pt-terminated film, ground state remains in AFM-II state as that in bulk. The layer-by-layer magnetism is briefly discussed to understand the respective magnetic ground states in the film structures. Both AFM-II and AFM-III states show in-plane magnetization in bulk structure. In the Mn-terminated film, AFM-III(AFM-II) shows out-of-plane (in-plane) magnetization. To provide the physical origin of different magnetization directions in both states we analyze the orbital resolved band structures and follow the same recipe as suggested by D. S. Wang et al. [27]. In the Pt-termination except for the 3 ML film, both AFM-II and AFM-III states show in-plane magnetization. In the presence of the substrate, interface effect plays a key role in the enhancement of MCA.

2. Computational method

Density functional calculations were performed using Vienna *ab initio* Simulation Package (VASP) [22]. The generalized gradient approximation (GGA) is employed for the exchange-correlation interaction within the projector augmented-waves scheme [23]. Energy cutoff of 450 eV is used for the wave function expansion, and the *k* meshes of 12 × 12 × 14 and 23 × 23 × 1 in the Monkhorst-Pack scheme are adopted for Brillouin zone integration of the bulk and the film structure, respectively. In the film calculations, a vacuum region of 15 Å was

* Corresponding author.
E-mail addresses: sonny@ulsan.ac.kr (S.H. Rhim), schong@ulsan.ac.kr (S.C. Hong).

https://doi.org/10.1016/j.jmmm.2018.07.055
Received 14 February 2018; Received in revised form 13 June 2018; Accepted 16 July 2018
Available online 21 July 2018
0304-8853/

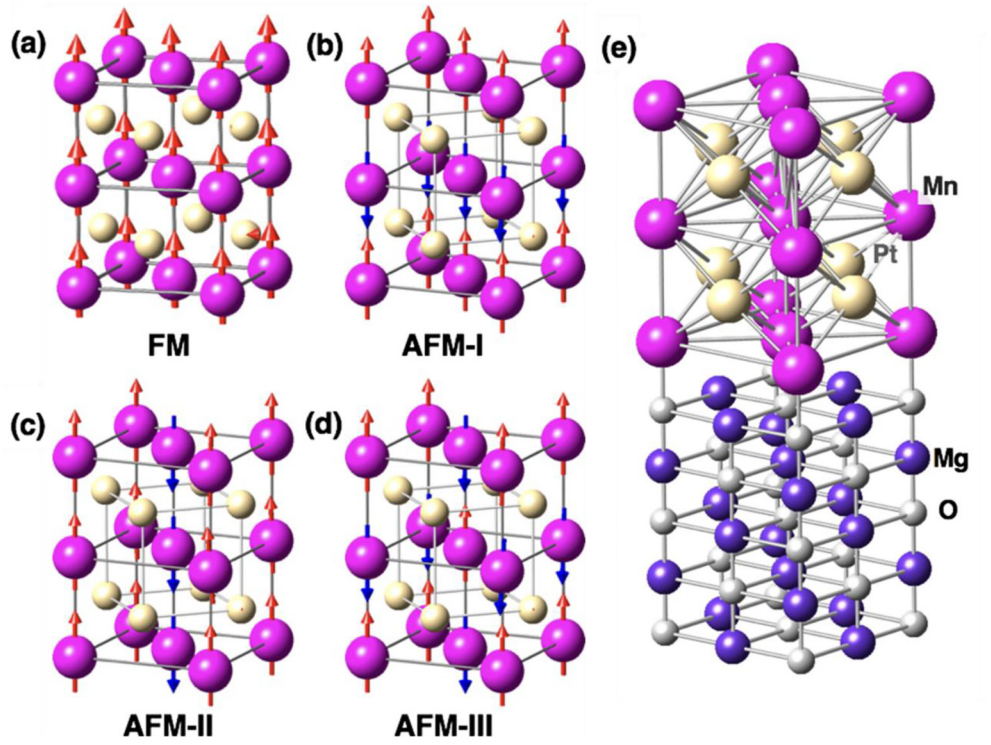

Fig. 1. Magnetic $L1_0$ unit cells of bulk MnPt doubled along the *c*-axis, (a) FM, (b) AFM-I; (c) AFM-II, (d) AFM-III, and (e) 5 ML Mn-terminated MnPt/MgO(0 0 1). Purple spheres with red (blue) arrows indicate the Mn atoms with spin-up (-down) while grey spheres do the Pt atoms. (For interpretation of the references to color in this figure legend, the reader is referred to the web version of this article.)

taken along the *z*-axis to eliminate any spurious interaction between adjacent slabs and the atomic positions along [0 0 1] are relaxed until the forces acting on the ions become $< 1 \times 10^{-3}$ eV/Å. MCA energy is calculated using the second-variation method employing the scalar-relativistic eigen functions and a $31 \times 31 \times 1$ ($17 \times 17 \times 19$) k-point mesh for film (bulk) structure. The MCA energy is determined by the total energy differences between two magnetization directions, $E_{MCA} = E_{(100)} - E_{(001)}$ within self-consistent scheme, where positive (negative) value indicates perpendicular (parallel) magnetization to the surface normal. The convergence test for self-consistent and MCA calculations with respect to cutoff energies and the number of k-points are carefully checked.

We studied four different magnetic structures in bulk MnPt, i.e. FM, AFM-I, AFM-II, and AFM-III. As shown in Fig. 1, AFM-I has FM configuration on the *xy*-plane and AFM one along the *z*-axis [see Fig. 1(b)]. Both of AFM-II and AFM-III have $c(1 \times 1)$ check-board AFM configurations on the *xy*-plane [see Fig. 1(c) and (d)], but the AFM-II and AFM-III have different magnetic couplings along the *z*-axis, FM in AFM-II and AFM in AFM-III, respectively. To account for the bulk AFM structures, a tetragonal $L1_0$ magnetic unit cell is taken by doubling along the *z*-axis. To study surface-termination- and thickness-dependent magnetism of the MnPt (0 0 1) films, Mn- and Pt-terminations with thickness (n) from 3 to 11 ML are considered. We do structural relaxation for the z-coordinates of the atoms while keeping in-plane lattice parameter fixed (lattice constant being listed in Table 1). To investigate interface effect on MCA we also consider 5 ML MnPt(0 0 1) film on 6 ML MgO(0 0 1) substrate with two Mn-O and Pt-O interfaces, as shown in Fig. 1(e). For the MnPt/MgO(0 0 1) film, an experimental lattice constant of MgO (4.238 Å) is adopted as the in-plane lattice constant of the thin film which matches within 2.17–3.36% to the optimized bulk MnPt lattices in all considered magnetic states.

3. Results and discussion

Bulk MnPt has an AFM-II magnetic ground state. The magnetic moments and structural parameter for all the considered magnetic structures are listed in Table 1, which are in good agreement with experimental data [19] and are also comparable with other theoretical calculations [24–26]. AFM-I and FM are higher in energies with the energy difference of about 0.120 and 0.144 meV/Mn from the AFM-II phase. While energy difference of AFM-III from AFM-II is significantly small, 0.034 meV/Mn. Therefore, for the thin film magnetism we focus more on AFM-II and AFM-III states. Magnetic moment of the Mn atom is 3.75 μ_B (3.71 μ_B) for AFM-II (AFM-III) and local moments of the Pt atom are zero in the AFM magnetic structures.

Moving on to the thin film magnetism, Fig. 2 represents the energy difference with respect to AFM-II phase for the Mn- and Pt-terminated (0 0 1) thin film: $\Delta E = E_{(Y)} - E_{(AFM\text{-}II)}$, (Y = FM, AFM-I, AFM-III). Clearly as shown in Fig. 2(a), thickness of the Mn-terminated film plays an important role in determining the magnetic ground state. For the film

Table 1
Calculated equilibrium lattice parameters, *a* (Å) and c/*a*, magnetic moment (μ) of Mn and Pt atoms(in μ_B), total energy difference (meV/Mn), $\Delta E = E_{(Y)} - E_{(AFM\text{-}II)}$, where Y = FM, AFM-I, and AFM-III.

AFM-I		AFM-II		AFM-III		FM	
Present	previous[26]	Present	previous[26]	Present	Previous	Present	Previous[26]
a	4.12	4.10	4.09	4.0	4.10	4.144.1	
c/*a*	0.87	0.87	0.89	0.92	0.88	0.86	0.92
$\mu_{(Mn)}$	3.81	3.89	3.75	3.80	3.71	3.83	3.94
$\mu_{(Pt)}$	0.00	0.00	0.09	0.00	0.00	0.39	0.39
ΔE	0.12	0.00	0.034	0.144			